Available online at www.sciencedirect.com
SCIENCE DIRECT
Journal of Power Sources 156 (2006) 166–170
JOURNAL OF POWER SOURCES
www.elsevier.com/locate/jpowsour

Synthesis and decomposition reactions of metal amides in metal–N–H hydrogen storage system

H.Y. Leng [a,*], T. Ichikawa [a,b], S. Hino [b], N. Hanada [b], S. Isobe [b], H. Fujii [a,b]

[a] *Materials Research Center, N-BARD, Hiroshima University, 1-3-1 Kagamiyama, Higashi-Hiroshima 739-8526, Japan*
[b] *Graduate School of Advanced Sciences of Matter, Hiroshima University, 1-3-1 Kagamiyama, Higashi-Hiroshima 739-8530, Japan*

Received 27 December 2004; received in revised form 18 March 2005; accepted 25 March 2005
Available online 13 June 2005

Abstract

The synthesis and decomposition properties of some metal amides $M(NH_2)_x$ such as $LiNH_2$, $NaNH_2$, $Mg(NH_2)_2$ and $Ca(NH_2)_2$ were investigated, which play important roles for designing a new family of metal–N–H hydrogen storage systems. Both the gas chromatographic examination and X-ray diffraction measurement indicated that the reaction between alkali or alkaline earth metal hydride MH_x (such as LiH, NaH, MgH_2 and CaH_2) and gaseous NH_3 could quickly proceed at room temperature by ball milling and the corresponding metal amides were easily synthesized in high quality. The kinetics of these kind of reactions is faster in the order of $NaH > LiH > CaH_2 > MgH_2$, which is consistent with the inverse order of electronegativity of those metals, i.e. $Na < Li = Ca < Mg$. The thermal decomposition properties indicated that both $Mg(NH_2)_2$ and $Ca(NH_2)_2$ decomposed and emitted NH_3 at lower temperature than $LiNH_2$.

Keywords: Hydrogen storage; Metal hydride; Ammonia; Metal amide; Reactive ball milling

1. Introduction

As early as 1910, Dafert and Miklauz [1] had reported that the reaction between lithium nitride Li_3N and hydrogen H_2 had generated Li_3NH_4, which was later proved to be a mixture of lithium amide $LiNH_2$ (1 mol) and lithium hydride LiH (2 mol) by Ruff and Goeres [2]. After almost 1 century, Chen et al. [3] and Hu and Ruckenstein [4] have investigated the system Li_3N as one of the hydrogen storage materials, where the hydrogenation and dehydrogenation of Li_3N were reversibly performed by the following two-step reversible reactions [3]:

$$Li_3N + 2H_2 \leftrightarrow Li_2NH + LiH + H_2 \leftrightarrow LiNH_2 + 2LiH \quad (1)$$

According to the two-step reactions in reaction (1), Li_3N can theoretically store 10.4 wt.% hydrogen. However, the standard enthalpy change (~148 kJ mol^{-1} H_2 [5]) of the desorption reaction at the first step is so high that a very high temperature over 430 °C [4] is required for the complete recovery of Li_3N from the hydrogenated state. On the other hand, since the second step reaction has much lower standard enthalpy change (44.5 kJ mol^{-1} H_2) of desorption and has still large amount of hydrogen capacity (6.5 wt.%), it is worthy to be studied as one of the rechargeable hydrogen storage system, which is expressed as follows:

$$LiNH_2 + LiH \leftrightarrow Li_2NH + H_2 \quad (2)$$

Ichikawa et al. [6] reported that the mixture of $LiNH_2$ and LiH doped with 1 mol% $TiCl_3$ by ball milling method reversibly desorbed and absorbed a large amount of hydrogen (~5.5 wt.%) in the temperature range from 150 to 200 °C. Furthermore, the mechanism of desorption reaction (2) was experimentally examined in detail [5,7], and the desorption has been clarified to proceed by the following two elementary reactions:

$$2LiNH_2 \rightarrow Li_2NH + NH_3 \quad (3)$$

* Corresponding author. Tel. +81 82 424 5744; fax: +81 82 424 7486.
E-mail address: hyleng@hiroshima-u.ac.jp (H.Y. Leng).

0378-7753/$ – see front matter © 2005 Elsevier B.V. All rights reserved.
doi:10.1016/j.jpowsour.2005.03.228

$$LiH + NH_3 \rightarrow LiNH_2 + H_2 \quad (4)$$

The reaction (3) is endothermic while the reaction (4) is exothermic which has been proved to be ultra-fast in the hydrogen desorption reaction (2) [7].

Some elements, especially those in groups of I–IV in the periodic table, can form their nitride, hydride and amide/imides. Among them, it still is possible to design plenty of metal–N–H systems with similar reactions to Eqs. (1) and (2), which are expected to be candidates for hydrogen storage. Quite recently, some new metal–N–H systems for hydrogen storage have been developed, such as the system composed of magnesium amide $Mg(NH_2)_2$ and LiH [8–11], the system composed of $Mg(NH_2)_2$ and MgH_2 [11,12], the system of Li–Ca–N–H [9] and so on. The hydrogen storage properties of those systems are quite different among them. For instance, the system composed of $Mg(NH_2)_2$ and LiH has much higher equilibrium pressure for hydrogen desorption than the system of $LiNH_2$ and LiH [9]. In order to understand the differences among them and to further develop the metal–N–H system as a new family of H-storage materials, the investigations on the reactions between metal hydrides and NH_3 and on the decomposition behaviors of the metal amides are very important and indispensable.

In this work, we investigated the novel reaction between MH_x and NH_3 at room temperature by mechanically milling, by which the corresponding metal amides could be effectively produced in high purity. Then, we examined the thermal decomposition behaviors of these metal amides.

2. Experimental

The starting materials were purchased from Sigma–Aldrich. LiH and NaH with 95% purity and MgH_2 with 90% purity (most of the impurities is no-hydrogenated Mg) and CaH_2 with 99.99% purity. All the material handlings (including weighing and loading) were performed in a glove-box filled with purified argon to keep a low water vapor concentration and a low oxygen concentration (less than 2 ppm for both) during operation using a gas recycling purification system (MP-P60W, Miwa MFG Co., Ltd.). One-hundred milligram samples and 20 steel balls of 7 mm in diameter were put into a milling vessel made of hardened Cr-steel, in which 0.4 MPa NH_3 gas was filled. The ball milling was performed using a rocking mill (RM-10, SEIWA GIKEN Co., Ltd.) with a frequency of 10 Hz. To avoid an increase in temperature during milling, the milling process was interrupted every 15 min. The fraction of H_2 in the milling vessel was monitored by gas chromatographic analysis (GCA) (Shimadzu, GC8AIT). The milling vessel was refilled with 0.4 MPa NH_3 every time after degassing until the reaction of metal hydrides with gaseous NH_3 was complete.

The quality of the products after milling was checked by X-ray diffraction (XRD) with Cu Kα radiation (Rigaku, RINT-2500) and elementary analysis due to oxygen combustion (Perkin-Elmer 2400α CHN).

The thermal decomposition behaviors of the products were examined by thermal desorption mass spectroscopy (TDMS) (Anelva M-QA200TS) combined with thermogravimetry (TG) in the heating process up to 500 °C at a heating rate of 5 °C min^{-1} under a helium flow. This equipment has been specially set inside the glove-box filled with purified argon, which permitted simultaneous measurements of TG and TDMS without exposing the samples to any air.

3. Results and discussion

3.1. Reaction between metal hydride and NH_3 by ball milling

Motivated by the reaction (4) between LiH and NH_3, we expected that the reactions between the alkali and alkaline earth metal hydrides and gaseous NH_3 would proceed by ball milling at room temperature according to the following reaction:

$$MH_x + xNH_3 \rightarrow M(NH_2)_x + xH_2 \quad (5)$$

where M represents alkali or alkaline earth metals like M = Li, Na, Mg or Ca. Fig. 1 shows the kinetic properties of the reactions between MH_x and NH_3. The time for the completion of the reaction (5) was estimated to be 1, 2, 8 and 13 h for NaH, LiH, CaH_2 and MgH_2, respectively. This indicates that the reaction rate is faster in the order of NaH > LiH > CaH_2 > MgH_2, being consistent with the inverse order of magnitude of those metals' electronegativities, i.e. Na < Li = Ca < Mg.

To confirm whether the corresponding metal amides were really synthesized in high quality, the products were examined by the XRD measurement. As shown in Fig. 2a, b and d, it is noticeable that the XRD patterns of the products are assigned to be almost single-phases of the corresponding

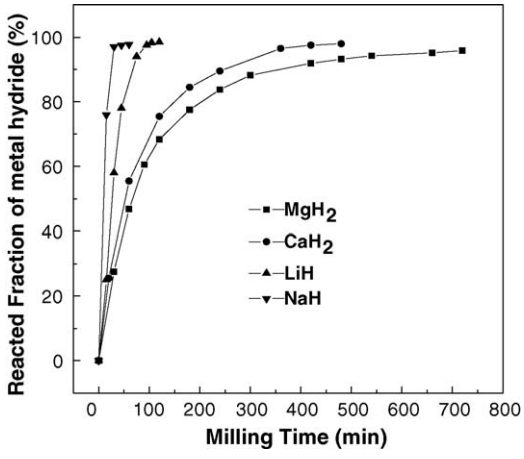

Fig. 1. Kinetic curves of the reactions between metal hydrides and NH_3 analyzed by GCA method.

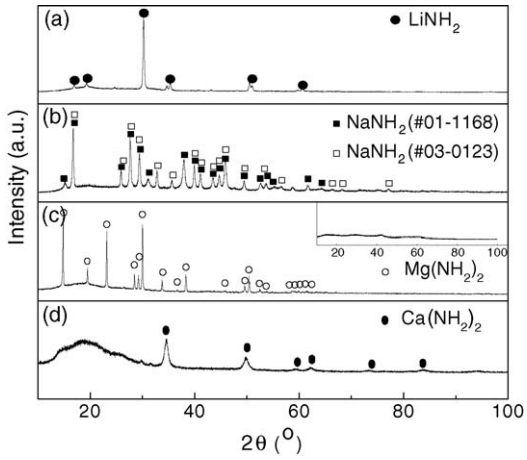

Fig. 2. XRD patterns of the products obtained (a) by milling LiH under 0.4 MPa NH_3 for 2 h; (b) by milling NaH under 0.4 MPa NH_3 for 1 h; (c) by milling MgH_2 under 0.4 MPa NH_3 for 13 h (the inserted one) and then by annealing the sample at 300 °C in NH_3 for 1 h; (d) by milling CaH_2 under 0.4 MPa NH_3 for 8 h. The symbols of #01-1168 and #03-0123 are the numbers of JCPDS file. The broad peak around 20° is due to grease using for fixing the powder on the sample holder.

metal amides $LiNH_2$, $NaNH_2$ and $Ca(NH_2)_2$, respectively. On the other hand, the X-ray pattern for the product prepared by milling MgH_2 under NH_3 for 13 h (Fig. 2c) shows a nano-structured or an amorphous phase because of showing no structural profile in it. Here, it is noted that the amorphous-like background around 20° in all the XRD patterns is from the grease using for fixing the powder on the sample holder. Since it was difficult to confirm the formation of the $Mg(NH_2)_2$ molecule by XRD, the elementary analysis was employed to chemically analyze the concentrations of H and N in the products. The mass ratio of N to H was estimated to be 7.0 ± 0.2 wt.%, which was in good agreement with the theoretical value of 6.95 expected for $Mg(NH_2)_2$ molecule. In addition, the product after heat treatment at 300 °C for 1 h under NH_3 atmosphere was confirmed to be the single phase of crystallized $Mg(NH_2)_2$ which is shown in Fig. 2c. Thus, the above results suggest that the product after ball milling is a nano-structured $Mg(NH_2)_2$ phase.

Generally, the light metal hydrides like LiH, NaH, MgH_2 and CaH_2 possess relatively high H densities among metal hydrides (12.7 wt.% in LiH, 4.2 wt.% in NaH, 7.7 wt.% in MgH_2 and 4.8 wt.% in CaH_2). However, their metal–H ionic-bonds are so strong that it requires quite high temperatures to complete their thermal decompositions (720 °C for LiH, 425 °C for NaH, 327 °C for MgH_2 and 650 °C for CaH_2) [13,14]. Nevertheless, their extremely stable chemical bonds between metals and hydrogen are easily loosed and broken because of the interaction with the polar molecule of NH_3, and the ionic metal hydrides exothermically react with NH_3 into their amides and gaseous hydrogen.

In order to examine how the milling process is vital for the present synthetic technique compared with the conventional synthesizing method of metal amides by heating the pure metals under NH_3 atmosphere [15,16], we carried out the following experiments. At the first step, LiH was kept under a 0.4 MPa NH_3 gas atmosphere for 3 h at room temperature under a static condition, but no H_2 was detected in the vessel by the GCA examination, indicating no proceeding of the reaction. At the next step, the sample was exposed to 0.4 MPa NH_3 gas for 3 h at 100 °C also under the static condition, but only about 1.5% H_2 was detected, indicating that only 1.5% of LiH reacts with NH_3 within 3 h at 100 °C. Thus, our experimental results indicated that it needs a very long time for proceeding of the reaction (4) without ball milling treatment at room temperature. This may be due to the fact that $LiNH_2$ is first formed on the surface layer of LiH particles by reacting with NH_3 and then NH_3 should diffuse through the $LiNH_2$ surface layer to further progress the reaction with LiH located inside the particle, which would take a long time to complete the reaction. On the other hand, when LiH was mechanically milled under a 0.4 MPa NH_3 gas atmosphere at room temperature, ~50% of LiH reacted with NH_3 even within 30 min (see Fig. 1). This indicates that the milling treatment leads to the acceleration of the reaction between the metal hydrides and gaseous NH_3, because the milling process can bring continuous creation of fresh reactive surfaces between metal hydrides and NH_3. Similarly, Dennis and Browne had reported that the bubbling of the ammonia through the molten sodium to increase the surface contact between the metals and gaseous NH_3, instead of merely conducting the gas over the surface of the metal, can greatly accelerate their interaction [15], which might bring similar effect to the milling treatment. However, this new technique brings no troubles caused by the melting of metals or metal amides [16], it can be developed as one of the effective methods for the synthesis of metal amides.

3.2. Decomposition reaction of metal amides

Next, the thermal decomposition properties were examined for the above metal amides. Fig. 3 shows TDMS and TG profiles obtained by heating up to 500 °C under a heating rate of 5 °C min^{-1} for the products except $NaNH_2$. In our experiments, $NaNH_2$ did not decompose into its imide in the heating process up to 300 °C. Since it easily reacted with the sample holders made of Au and Al metals, and melted and/or volatilized at higher temperatures, another suitable method is needed to clarify the decomposition behavior of $NaNH_2$ at higher temperatures.

As shown in Fig. 3a, the NH_3 desorption reaction from $LiNH_2$ prepared by ball milling for 2 h begins around 220 °C and the TDMS profile shows clear double peaks around 320 and 400 °C. The weight loss due to the NH_3 desorption is ~37 wt.% up to 500 °C, which should correspond to the decomposition of $2LiNH_2$ into Li_2NH and NH_3. The XRD profile also indicates that $LiNH_2$ fully transforms into Li_2NH after decomposition within 500 °C (Fig. 4a). Furthermore, we examined the decomposition of the sample at 320 °C corresponding to the first peak in Fig. 3a under helium flow for 2 h. The results showed that the weight loss due to the NH_3

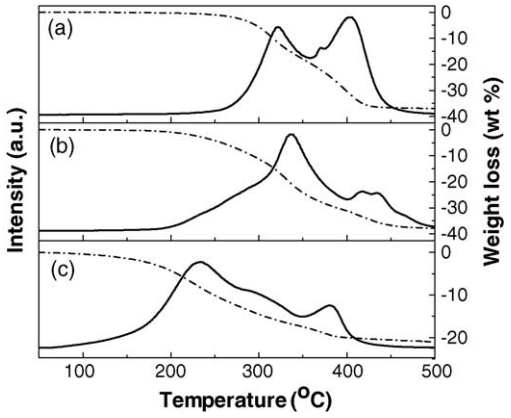

Fig. 3. Thermal desorption mass spectrum (solid lines) and thermogravimetry profiles (dashed lines) of the metal amides during the heating process up to 500 °C at a 5 °C min^{-1} heating rate under a helium flow. (a) $LiNH_2$ made by milling LiH under 0.4 MPa NH_3 for 2 h; (b) $Mg(NH_2)_2$ produced by milling MgH_2 under 0.4 MPa NH_3 for 13 h; (c) $Ca(NH_2)_2$ synthesized by milling CaH_2 under NH_3 for 8 h.

emission reached up to ~35 wt.% and the XRD profile also showed the same structure as that in Fig. 4a. Therefore, both two peaks in the NH_3 desorption profile should correspond to the decompositions from $LiNH_2$ to Li_2NH and be originated in some kinetic characters.

As is shown in Fig. 3b, the NH_3 gas is desorbed from $Mg(NH_2)_2$ at a temperature above 175 °C and the desorption profile shows two peaks around 335 and 420 °C on the heating process up to 500 °C. However, the origin of appearing

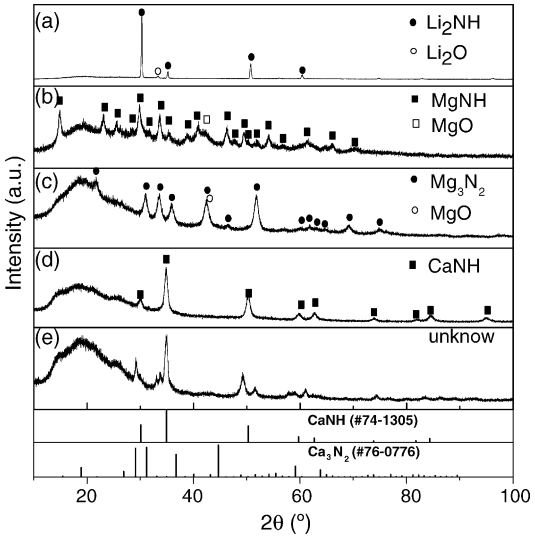

Fig. 4. XRD patterns of the products after thermal decomposition (a) the product of $LiNH_2$ after heating up to 500 °C under a helium flow; (b) the product of $Mg(NH_2)_2$ after thermal desorption under a helium flow at 340 °C for 2 h; (c) the product of $Mg(NH_2)_2$ after heating up to 500 °C under a helium flow; (d) the product of $Ca(NH_2)_2$ after heating up to 350 °C under a helium flow; (e) the product of $Ca(NH_2)_2$ after heating up to 500 °C under a helium flow. The JCPDS profiles of CaNH and Ca_3N_2 are shown in the below for comparison. The broad peak around 20° is due to grease using for fixing the powder on the sample holder.

two-peak structure in the NH_3 desorption from $Mg(NH_2)_2$ is different from that of the $LiNH_2$ case. It may be due to the existence of two-step chemical reactions, because the XRD profile of the product after thermal desorption at 340 °C for 2 h under helium flow was assigned to MgNH phase (Fig. 4b), but it transformed into Mg_3N_2 phase after the thermal desorption up to 500 °C (Fig. 4c). Therefore, the weight loss of ~30 wt.% due to the first step desorption of NH_3 up to around 400 °C mainly corresponded to the decomposition from $3Mg(NH_2)_2$ to 3MgNH and $3NH_3$, while the second step desorption of NH_3 leading the total weight loss up to ~40 wt.% until 500 °C, mainly corresponded to the decomposition of 3MgNH into Mg_3N_2 and NH_3.

The decomposition behavior from $Ca(NH_2)_2$ is shown in Fig. 3c as well. We notice that the NH_3 gas is emitted from 70 °C and the desorption curve takes two main peaks at 230 and 380 °C, respectively. According to the weight loss percent of 21%, the product after heating up to 500 °C should be a CaNH phase. However, the XRD profile cannot be assigned to a well-known cubic CaNH phase (Fig. 4e). On the other hand, when the $Ca(NH_2)_2$ was heated up to 350 °C which corresponds to weight loss of 16.0 wt.% in Fig. 3c, the product could be assigned to the cubic CaNH phase (Fig. 4d). This suggests that an unknown phase transition took place during the decomposition of $Ca(NH_2)_2$ within 500 °C. The phase changes in Ca–N–H are reported in detail elsewhere [17]. At present, it is still out of our understanding of the complicated decomposition behavior of $Ca(NH_2)_2$, which is similar to the complicated behavior in the reaction between Ca_3N_2 and H_2 [14]. Further investigation is needed to clarify the decomposition mechanism in the system of Ca–N–H.

Comparing the decomposition behaviors, it is noticeable that both the $Mg(NH_2)_2$ and $Ca(NH_2)_2$ are more unstable than $LiNH_2$ in the thermodynamic and kinetic point of view. Generally, the electronegativity of metal can affect the decomposition behavior of the corresponding metal amide. In fact, since the electronegativity of Mg is larger than that of Li, the ionic bond between the cation Mg^{2+} and anion $[NH_2]^-$ would be weaker than that between Li^+ and $[NH_2]^-$ ions. This well explains the results of lower temperature decomposition and slower synthesis of $Mg(NH_2)_2$ compared with $LiNH_2$ in this work. Furthermore, it is noteworthy that $Mg(NH_2)_2$ decomposes into MgNH and finally into Mg_3N_2 within 500 °C, while $LiNH_2$ decomposes not into Li_3N but Li_2NH in the same condition.

On the other hand, $Ca(NH_2)_2$ shows unusual decomposition behaviors from the viewpoint of electronegativity of metal. Because the electronegativity of Ca is smaller than that of Mg, the bond between the Ca^{2+} and $[NH_2]^-$ should be stronger than that between Mg^{2+} and $[NH_2]^-$, which might qualitatively explain the difference of kinetic behavior of the reactions between CaH_2/MgH_2 and NH_3 shown in Fig. 1. However, the decomposition behavior that the NH_3 desorption temperature from $Ca(NH_2)_2$ is much lower than that from $Mg(NH_2)_2$ (Fig. 3b and c) is not simply understood through the consideration of the electronegativity. This

indicates that the other factors controlling the activation energy for the progress of decomposition should be considered for understanding the decomposition behavior for the amides.

According to the hydrogen desorption mechanism of $LiNH_2$ and LiH system where the decomposition reaction (3) of $LiNH_2$ is the first elementary step [5], it is expected that if the metal amide more easily decomposes and emits ammonia, the hydrogen desorption properties will be much more improved. Therefore, the mixed $Mg(NH_2)_2$ and MH_x system would be recognized as one of the promising metal–N–H systems for hydrogen storage. In fact, the metal–N–H system composed of $Mg(NH_2)_2$ and LiH showed a quicker hydrogen desorption property at lower temperature than that of $LiNH_2$ and LiH [8–12]. Similarly, according to the second elementary step reaction (4), the reaction between metal hydride and NH_3 will also effect the hydrogen desorption properties of the metal–N–H system. That is to say, the faster reaction between metal hydride and NH_3 can effectively transform into the corresponding metal amide and desorb hydrogen, leading to the better hydrogen storage properties. For example, since the reaction between LiH and NH_3 is faster than that of MgH_2 and NH_3, the hydrogen desorption kinetics in the system composed of 8LiH and $3Mg(NH_2)_2$ is much better than that in the system of $2MgH_2$ and $Mg(NH_2)_2$ [12].

4. Conclusions

The reaction between MH_x and gaseous NH_3 was confirmed to proceed quickly at room temperature by ball milling and the resultant product is the corresponding metal amide $M(NH_2)_x$ (M = Na, Li, Mg or Ca), because the milling treatment leads to the acceleration of the reaction between the metal hydrides and gaseous NH_3 by continuous creation of fresh reactive surfaces between metal hydrides and NH_3. The kinetics of the reaction between MH_x and NH_3 by ball milling is faster in the order of $NaH > LiH > CaH_2 > MgH_2$, which is consistent with the inverse order of electronegativity of metals, i.e. $Na < Li = Ca < Mg$. On the other hand, compared with $LiNH_2$, both $Mg(NH_2)_2$ and $Ca(NH_2)_2$ more easily decomposed and emitted NH_3 at lower temperature. Furthermore, $Mg(NH_2)_2$ decomposed into its nitride within 500 °C while $LiNH_2$ only decomposed into its imide in the same temperature range.

Acknowledgements

This work was supported by the Grant-in-Aid of Japan Society for the Promotion of Science, by the project "Development for Safe Utilization and Infrastructure of Hydrogen Industrial Technology" of the New Energy and Industrial Technology Development Organization (NEDO), and by COE Research program (No. 13CE2002) of the Ministry of Education, Culture, Sports, Sciences and Technology of Japan. The authors gratefully acknowledge Miss E. Gomibuchi, Mr. K. Nabeta, Mr. K. Kimura, and Mr. T. Nakagawa for their help in our laboratory.

References

[1] F.W. Dafert, R. Miklauz, Monatsh. Chem. 31 (1910) 981–996.
[2] O. Ruff, H. Goeres, Chem. Ber. 44 (1910) 502–506.
[3] P. Chen, Z. Xiong, J. Luo, J. Lin, K.L. Tan, Nature 420 (2002) 302–304.
[4] Y.H. Hu, E. Ruckenstein, Ind. Eng. Chem. Res. 42 (2003) 5135–5139.
[5] T. Ichikawa, N. Hanada, S. Isobe, H.Y. Leng, H. Fujii, J. Phys. Chem. B 108 (2004) 7887–7982.
[6] T. Ichikawa, S. Isobe, N. Hanada, H. Fujii, J. Alloys Compd. 365 (2004) 271–276.
[7] Y.H. Hu, E. Ruckenstein, J. Phys. Chem. A 107 (2003) 9737–9739.
[8] H.Y. Leng, T. Ichikawa, S. Hino, N. Hanada, S. Isobe, H. Fujii, J. Phys. Chem. B 108 (2004) 8763–8765.
[9] Z. Xiong, G. Wu, J. Hu, P. Chen, Adv. Mater. 16 (2004) 1522–1525.
[10] Y. Nakamori, G. Kitahara, K. Miwa, S. Towata, S. Orimo, Appl. Phys. A 80 (2005) 1–3.
[11] Y. Nakamori, G. Kitahara, S. Orimo, J. Power Sources 138 (2004) 309–312.
[12] H.Y. Leng, T. Ichikawa, S. Isobe, S. Hino, H. Hanada, H. Fujii, J. Alloys Compd., in press.
[13] W. Grochala, P.P. Edwards, Chem. Rev. 104 (2004) 1283–1315.
[14] Z. Xiong, P. Chen, G. Wu, J. Lin, K.L. Tan, J. Mater. Chem. 13 (2003) 1676–1680.
[15] L.M. Dennis, A.W. Browne, J. Am. Chem. Soc. 26 (1904) 587–600.
[16] F.W. Bergstrom, W.C. Fernelius, Chem. Rev. 12 (1933) 43–167.
[17] S. Hino, T. Ichikawa, H.Y. Leng, H. Fujii, J. Alloys Compd., in press.